Relational Reconstruction of Spacetime Geometry from Graph Laplacians

Jérôme Beau[1*]

[1*]Independent Researcher, France.

Corresponding author(s). E-mail(s): jerome.beau@cosmochrony.org;

Abstract

Background: We develop a relational and spectral framework in which metric geometry emerges from correlation structures alone, without assuming a background manifold, coordinates, or fundamental geometric degrees of freedom.
Methods: Starting from a relational substrate equipped with a symmetric connectivity operator, we define operational distances via minimal path functionals and introduce a non-circular coarse-graining scheme separating combinatorial neighborhoods from geometry-aware weighted distances. Spectral admissibility criteria identify regimes supporting a stable continuum approximation.
Results: In these projectable regimes, the distance matrix admits a low-dimensional embedding, yielding emergent coordinates and an effective metric structure. Proper time, spatial distance, and curvature arise as coarse-grained summaries of relational organization. In symmetric weak-field limits, the effective metric reproduces Schwarzschild geometry without postulating fundamental gravitational dynamics.
Conclusions: Breakdown of geometry occurs when spectral gaps close or connectivity becomes non-local, providing intrinsic limits to continuum spacetime. Analytical and numerical benchmarks establish robust spectral invariants, including the $\mathbf{8/3}$ eigenvalue ratio on $\boldsymbol{S^3}$. Spacetime thus appears as an operational construct emerging from relational spectral structure rather than a primitive entity.

Keywords: Pre-geometric substrate, emergent spacetime, relational dynamics, spectral geometry, emergent metric, spectral dimension

Contents

1 Introduction **3**

2 Relational Substrate and Spectral Structure **4**
2.1 Relational Structure 4

3 Spectral Distance and Embedding **5**
3.1 Spectral proximity 5
3.2 Spectral distance 5
3.3 Local embedding and quadratic approximation 6
3.4 Scope and limitations 6

4 Continuum Limit and Emergent Metric **7**
4.1 Spectral Admissibility and Regularity 7

5 Operational Geometry **8**
5.1 Collective Coupling and Operational Geometry 8
5.2 Emergent Curvature 9
5.3 Static Spherically Symmetric Geometry 10

6 GR Limit: Schwarzschild-type Recovery **10**
6.1 Non-uniqueness of Spectral Reconstruction 10
6.2 Validity of Geometric Descriptions 11
6.3 Limits of Schwarzschild-Type Reconstruction 11

7 Discussion **12**
7.1 Structural robustness beyond geometric descriptions 12
7.2 Status of spacetime geometry 12
7.3 Relation to existing approaches 13
7.4 Non-uniqueness and regime dependence 13
7.5 Spectral rigidity and structural invariants 14
7.6 Scope and limitations 14
7.7 Outlook 15

A Relational Distance as a Minimal Path Functional **16**
A.1 Combinatorial vs. weighted distance 16
A.2 Weight functional and positivity 17
A.3 Metric status 17

B Relation to the Effective Geometric Description **18**

C Emergent Coordinates via Manifold Reconstruction **18**
C.1 MDS embedding from relational distances 18
C.2 Intrinsic dimension from the eigenvalue gap 19
C.3 Breakdown as a physical prediction 19
C.4 Convergence of the relational weight construction in the dense graph limit 20

C.5 Analytical derivation of the spectral ratio on S^3 20
C.6 Example of a Robust Spectral Ratio in a Relational Laplacian 22

1 Introduction

A central problem in gravitational physics is the reconstruction of spacetime geometry from non-metric structures. In general relativity, the metric tensor is postulated as a fundamental dynamical field. In background-independent approaches, by contrast, geometry is expected to arise as an effective description reconstructed from relational or pre-geometric data.

Across canonical, covariant, causal-set, loop-based, and spectral programs, a common challenge persists: how to recover a smooth pseudo-Riemannian geometry from fundamentally non-metric degrees of freedom without assuming a background manifold or metric.

We address this reconstruction problem from a minimalist and operational perspective. We consider relational systems described by connectivity data encoded in discrete or coarse-grained graphs. The central object of analysis is the spectrum of a Laplacian operator defined on these relational structures. Our goal is to determine under which conditions spectral data alone suffice to define effective notions of distance, curvature, and geometry.

Spectral information provides a natural bridge between discrete relational systems and continuum geometry. In appropriate limits, graph Laplacian spectra encode geometric information analogous to that of differential operators on smooth manifolds. However, only a controlled portion of the spectrum contributes to the reconstruction of effective geometry. We make this correspondence explicit by formulating spectral admissibility conditions under which an effective metric structure can be reconstructed from the low-lying spectral sector without postulating coordinates, metric tensors, or variational principles.

Admissible relational configurations are characterized by spectral consistency criteria. Effective geometric quantities are reconstructed through spectral distances and embeddings defined purely from the Laplacian spectrum. An effective metric description arises only in regimes admitting a stable spectral continuum limit.

Within this framework, we show how local metric structure emerges, how curvature can be defined operationally, and how general-relativistic geometries are approximated in appropriate limits. The reconstruction exhibits a characteristic spectral rigidity: the lowest non-trivial eigenvalues organize according to a universal ratio $\lambda_2/\lambda_1 = 8/3$ associated with the S^3 structure of the admissible projection space. As a benchmark, we recover a Schwarzschild-type effective geometry from purely spectral and relational inputs.

The scope of this work is restricted to the geometric reconstruction problem. We do not address matter dynamics, quantum statistics, or cosmological evolution. The aim is not to construct a complete theory of quantum gravity, but to isolate and analyze the emergence of geometry in its minimal form.

Unlike standard spectral geometry approaches, which assume a manifold and study spectral properties of differential operators defined on it, the present framework proceeds

in the opposite direction. The relational operator is taken as the primitive object, and geometric structure is reconstructed from its spectrum without presupposing an underlying manifold or coordinate system. Geometry therefore appears as an emergent description of relational spectral structure rather than as a fundamental input.

Section 2 introduces the relational graph framework and associated Laplacian. Section 3 develops spectral notions of distance and embedding. Section 4 analyzes the emergence of effective continuum geometry. Section 5 defines curvature operationally, and Section 6 presents the Schwarzschild-type recovery. Technical derivations are collected in the appendices.

2 Relational Substrate and Spectral Structure

We introduce the minimal relational framework underlying the spectral constructions developed in this work. No spacetime manifold, metric tensor, or background geometry is assumed. The only primitive structure is a relational connectivity network from which a Laplacian operator can be defined.

We consider systems represented by discrete or coarse-grained graphs. Vertices correspond to abstract relational elements, and edges encode admissible relations. Graphs may be weighted or unweighted. No embedding space, coordinate chart, distance, dimension, or curvature is introduced at this stage.

Given an adjacency relation (possibly weighted), a graph Laplacian can be constructed following standard definitions in graph theory [1, 2]. This operator encodes the local connectivity structure of the system. Its spectrum constitutes the primary object of analysis.

The relational graphs are not interpreted as fundamental physical objects. They serve as minimal mathematical representations suitable for spectral analysis. Spectral reconstruction is generally non-injective, and distinct relational configurations may correspond to the same effective geometric description.

Geometric notions are introduced only at a secondary level through spectral constructions applied to families of admissible graphs. When appropriate regularity and consistency conditions are satisfied, these constructions admit continuum-like limits. The admissibility criteria and reconstruction procedures are developed in the following sections.

No dynamical, temporal, or causal assumptions are made at this stage. The framework is purely kinematic.

2.1 Relational Structure

We introduce a minimal relational framework capturing the weakest structural assumptions required for spectral reconstruction. No spacetime manifold, metric tensor, coordinate system, or causal structure is postulated.

The system consists of abstract relational elements together with admissible relations defining a connectivity structure, represented discretely or in coarse-grained form. No embedding space or background geometry is assumed.

Relational elements carry no intrinsic local values, dimensional quantities, or order parameters. Such quantities arise only at an effective level when the configuration

admits a stable spectral reconstruction. Distance, dimension, and curvature are therefore reconstructed descriptors, not primitives.

Spectral reconstruction is inherently non-injective: distinct relational configurations may yield identical effective geometries, and a single configuration may admit multiple equivalent spectral representations. This loss of information is structural and does not rely on physical coarse-graining.

Geometric and field-theoretic terminology is used only at the effective level, in regimes where a consistent spectral continuum approximation exists. It does not imply underlying spacetime entities or dynamical fields.

This relational starting point provides a neutral basis for defining spectral operators and investigating the emergence of geometric structure from connectivity data alone.

3 Spectral Distance and Embedding

A key step in geometric reconstruction is defining distance without assuming a pre-existing metric or coordinate structure. We introduce spectral notions of proximity and distance derived solely from the Laplacian of a relational graph.

Let the system be represented by a graph endowed with a Laplacian operator Δ. No embedding space or background geometry is assumed. The spectrum and eigenfunctions of Δ encode the connectivity structure and provide the only input for the constructions that follow. The relation between Laplacian spectra and global connectivity properties is standard in spectral graph theory [3].

3.1 Spectral proximity

Given the Laplacian spectrum $\{\lambda_n, \phi_n\}$, spectral kernels define relational proximity between nodes. A canonical example is the heat kernel

$$K(i,j;\alpha) \;=\; \sum_n e^{-\alpha\lambda_n}\,\phi_n(i)\,\phi_n(j), \tag{1}$$

where α sets the spectral scale.

This kernel measures connectivity between elements i and j through the spectrum of Δ, without reference to metric distance. Such constructions are standard in clustering and manifold learning [4]. They are invariant under node relabeling and require no embedding structure.

3.2 Spectral distance

From the spectral kernel, an effective distance is defined by

$$d_{\mathrm{spec}}(i,j) \;=\; -\log\left(\frac{K(i,j;\alpha)}{\sqrt{K(i,i;\alpha)\,K(j,j;\alpha)}}\right), \tag{2}$$

which is symmetric, non-negative, and vanishes for $i = j$. The definition is purely spectral and requires no geometric interpretation.

Spectral reconstruction is non-injective: distinct relational configurations may yield identical distance matrices, and multiple embeddings may correspond to the same d_{spec}. This non-uniqueness is structural.

Local embeddings, intrinsic dimension selection, and breakdown outside the projectable regime are detailed in Appendix C.

Emergent spectral dimension.

The exponent d appearing in Eq. (2) is not postulated as a topological dimension. It is extracted from the asymptotic scaling of the eigenvalue counting function $N(\lambda)$ in the low-energy regime, via the slope of $\log N(\lambda)$ versus $\log \lambda$. At finite resolution, d may be non-integer.

Under admissibility and regularity conditions, the relational substrate exhibits stable convergence toward $d \simeq 4$ across multiple spectral decades. This behavior is not imposed *a priori* and is robust across discretizations. Deviations at high spectral scales correspond to ultraviolet effects, where an effective geometric interpretation is not applicable.

From graph distance to effective geodesics.

Shortest weighted paths on the relational graph define an operational geodesic distance. Edge weights encode local connectivity variations, so path length reflects inhomogeneous relational structure.

In the continuum limit, the density of admissible nodes along paths controls volume and distance scaling. This density plays the role of a discrete analog of $\sqrt{-g}$, so geometric structure arises from connectivity statistics rather than a fundamental metric field.

3.3 Local embedding and quadratic approximation

When the relational system exhibits sufficient spectral regularity, the spectral distance matrix admits a local low-dimensional embedding. Auxiliary coordinates x^μ may then parameterize this embedding space.

For nearby elements, the spectral distance admits the quadratic approximation

$$d_{\mathrm{spec}}(i,j)^2 \;\approx\; g_{\mu\nu}(x)\,\Delta x^\mu \Delta x^\nu, \tag{3}$$

where $g_{\mu\nu}$ is a symmetric tensor summarizing the local spectral structure.

Such quadratic expansions and their relation to effective metric tensors are standard in metric geometry [5]. Here, $g_{\mu\nu}$ is not fundamental but arises as a local descriptor valid only in regimes where smooth spectral embedding exists. Outside these regimes, no metric interpretation is assumed.

3.4 Scope and limitations

The constructions developed here are purely kinematic. No assumptions on dynamics, temporal ordering, or causal structure are made. Their sole purpose is to reconstruct effective geometric notions from spectral data of relational connectivity.

Continuum limits, curvature reconstruction, and comparison with known geometric solutions are addressed in subsequent sections.

4 Continuum Limit and Emergent Metric

The spectral distance provides a relational notion of proximity. We now identify the conditions under which it admits a smooth continuum approximation and an effective metric description.

Consider families of relational graphs whose Laplacian spectra exhibit sufficient regularity. No manifold or dimensionality is assumed. The continuum regime is defined operationally as one in which spectral distances vary smoothly and admit consistent local approximations.

A central requirement is local factorizability: the relational system decomposes approximately into weakly coupled subsystems, enabling local definitions of spectral distance. This property underlies effective locality and permits the introduction of auxiliary coordinate charts.

Continuum reconstruction is non-unique. Spectral geometry is generically non-injective: distinct relational configurations may induce identical effective metrics, and a given configuration may admit multiple equivalent embeddings. This ambiguity is structural.

When factorizability and spectral regularity hold, the spectral distance admits the local quadratic form

$$d_{\mathrm{spec}}(i,j)^2 \;\approx\; g_{\mu\nu}(x)\,\Delta x^\mu \Delta x^\nu, \tag{4}$$

where $g_{\mu\nu}(x)$ summarizes the leading-order behavior of spectral distances. The metric tensor is derived, not fundamental.

The approximation is valid only when higher-order spectral corrections remain subdominant. Outside this regime, no smooth geometric interpretation is assumed.

The framework remains purely kinematic. No assumptions on dynamics, causality, or temporal ordering are required for metric emergence.

4.1 Spectral Admissibility and Regularity

An effective continuum geometry requires additional spectral regularity. Not all relational configurations admit a meaningful continuum approximation, even when a spectral distance exists. We therefore introduce spectral admissibility criteria.

Let L be a self-adjoint relational operator acting on a suitable Hilbert space. In discrete realizations, L reduces to a graph Laplacian. It encodes relational structure without reference to any manifold or metric.

The spectral decomposition

$$L\psi_n = \lambda_n \psi_n, \tag{5}$$

with non-negative eigenvalues $\{\lambda_n\}$, provides the basis for reconstruction.

Admissibility is defined by restricting attention to a controlled spectral window. We introduce a smooth spectral filter

$$F_{\lambda_*} \;=\; f\!\left(\frac{L}{\lambda_*}\right), \tag{6}$$

where $f(x)$ is a cutoff function and λ_* sets the characteristic scale. Only modes below λ_* contribute to the effective geometry.

Modes above the cutoff do not admit an independent geometric interpretation within the projected description. They remain confined to the unresolved sector of the relational configuration space and therefore cannot be represented as separable geometric observables. In the terminology adopted in later developments of the framework, such modes may be interpreted as *infra-projectable invariants*: degrees of freedom encoded in the projection fiber that remain invisible to the effective geometry.

In dense regular regimes satisfying the standard sampling assumptions of spectral graph convergence theory, the filtered operator $F_{\lambda_*}(L)$ converges in the strong resolvent sense to its continuum counterpart, equivalently implying convergence of low-lying eigenpairs up to the cutoff λ_*.

This criterion is purely spectral and does not rely on locality, coordinates, or integration measures. It reflects the insensitivity of continuum geometry to fine-grained spectral structure beyond a given resolution.

As before, spectral reconstruction is non-injective: distinct configurations may coincide within the admissible window, and a single configuration may admit multiple equivalent embeddings. This ambiguity is structural.

Admissibility conditions may involve monotonic spectral filters, reflecting the insensitivity of continuum structure to fine-grained spectral rearrangements beyond a given resolution.

The effective metric arises solely from relational spectral data and requires no additional fundamental fields.

5 Operational Geometry

5.1 Collective Coupling and Operational Geometry

Curvature in a relational framework arises as a collective effect. Geometric properties emerge from how relational variations influence one another across extended regions, without postulating a fundamental gravitational field.

In approximately homogeneous regimes, variations propagate uniformly. Localized irregularities modify this collective response, which can be summarized by an effective coupling characterizing the stiffness of the relational structure under relative deformations.

Distance is defined operationally: regions are proximate if relational variations can be efficiently correlated. In weakly inhomogeneous continuum regimes, this operational proximity admits a compact geometric representation. An effective metric summarizes the collective response of the system, without constituting an independent degree of freedom.

Curvature thus appears as a macroscopic descriptor of how localized relational structure modulates global connectivity.

Spectral convergence and continuum limit.

Under standard regularity assumptions (uniform density, bounded degree growth, approximate isotropy), the graph Laplacian Δ_G converges, in the strong resolvent sense, to a Laplace–Beltrami operator $\Delta_{\mathcal{M}}$ on an effective manifold $\mathcal{M}$.

Operationally, low-lying eigenmodes of Δ_G approximate those of $\Delta_{\mathcal{M}}$ below a spectral cutoff λ_*. Beyond this scale, smooth geometry ceases to apply. Such convergence results are well established in spectral graph theory and justify the continuum interpretation of the admissible spectral sector.

Spectral dimension as emergent observable.

Effective dimensionality is inferred from spectral data. Using the heat kernel

$$K(t) = \sum_n e^{-t\lambda_n}, \tag{7}$$

the spectral dimension is defined by

$$d_s(t) = -2\frac{d\log K(t)}{d\log t}. \tag{8}$$

In admissible regimes, $d_s(t)$ exhibits a stable large-scale plateau. Configurations relevant to the gravitational regime display $d_s \simeq 4$ robustly across discretizations, without imposing dimensionality *a priori*.

Role of the spectral scale λ_*.

The cutoff λ_* defines the upper limit of spectral admissibility. Above this scale, spectral locality breaks down and smooth geometric reconstruction becomes ill-defined.

This ultraviolet breakdown signals the transition to a pre-geometric regime rather than a failure of the framework.

5.2 Emergent Curvature

In the relational framework, curvature emerges as a collective descriptor of spatial variations in connectivity and spectral coupling. Non-uniform correlation patterns across extended regions, when a smooth parametrization is available, are summarized by gradients of an effective metric.

Curvature is not a fundamental dynamical field. It encodes how localized relational structure modulates collective connectivity. The metric serves as a compact representation of constrained relational organization in continuum regimes.

Within such regimes, the reconstructed curvature reproduces standard geometric phenomenology, including geodesic deviation, gravitational redshift, and lensing effects. These arise from variations in relational coupling, not from fundamental spacetime geometry.

Geometric language is therefore strictly operational. Outside smooth, slowly varying regimes, no metric interpretation is assumed.

5.3 Static Spherically Symmetric Geometry

Consider a static, approximately spherically symmetric relational configuration admitting a smooth continuum limit. The analysis is purely kinematic and constrained by symmetry and weak-field consistency.

The effective metric takes the standard form

$$ds^2 = -A(r)\,c^2dt^2 + B(r)\,dr^2 + r^2d\Omega^2, \tag{9}$$

where $A(r)$ and $B(r)$ encode the operational relation between temporal and spatial intervals.

In the weak-field regime,

$$A(r) \simeq 1 + 2\frac{\Phi(r)}{c^2}, \qquad B(r) \simeq \left(1 + 2\frac{\Phi(r)}{c^2}\right)^{-1}, \tag{10}$$

with $\Phi(r)$ characterizing deviations from flat geometry. No dynamical origin for Φ is assumed.

Imposing asymptotic flatness and spherical symmetry fixes the exterior solution at leading order,

$$A(r) = 1 - \frac{r_s}{r}, \qquad B(r) = \left(1 - \frac{r_s}{r}\right)^{-1}, \tag{11}$$

where r_s is an integration constant. This coincides with the Schwarzschild geometry at leading order.

Standard weak-field effects—gravitational redshift, light deflection, and time dilation—follow directly from the metric structure as kinematic consequences.

6 GR Limit: Schwarzschild-type Recovery

6.1 Non-uniqueness of Spectral Reconstruction

Reconstruction of an effective metric from spectral data is generically non-unique. This ambiguity is structural, not a consequence of approximation.

Distinct relational configurations may share identical low-resolution spectral content within an admissible window and therefore yield the same effective metric. Conversely, a given configuration may admit multiple spectrally equivalent continuum embeddings.

Because distance is defined operationally through spectral proximity, different filtering scales or embedding procedures can produce metrically equivalent but geometrically distinct descriptions. All such descriptions agree on observable properties within their common domain of validity. The effective metric thus represents an equivalence class compatible with the same spectral data.

Flux conservation and radial scaling.

The emergence of a $1/r$ profile follows from conservation of relational relaxation flux in quasi-static regimes. The total flux through any closed relational surface surrounding a localized perturbation is conserved.

In an effective three-dimensional projectable regime, flux conservation implies a $1/r^2$ decay of connectivity perturbations. Integration along admissible paths then yields an effective potential proportional to $1/r$. The Schwarzschild factor $1 - r_s/r$ thus arises from isotropic flux conservation rather than from an imposed force law.

Origin of the $1/r$ profile.

Mass corresponds operationally to a localized inhibition of admissible relaxation in the relational substrate. This reduces the density of optimal relational paths.

In the continuum regime, this reduction acts as a source term for the effective scalar Laplacian governing metric deformations. In three spatial dimensions, the corresponding Poisson equation has the unique fundamental solution proportional to $1/r$. The Schwarzschild scaling therefore follows from flux conservation in an isotropic effective geometry, not from an assumed gravitational law.

6.2 Validity of Geometric Descriptions

The emergence of curvature and metric structure does not imply universal validity of geometric descriptions. Geometry functions as an effective language, applicable only when the relational substrate admits a smooth and locally stable continuum approximation.

Within such regimes, geometric relations are robust: local curvature, geodesic deviation, and horizon structure depend weakly on microscopic relational details, explaining the observed universality of geometric behavior.

When injectivity or smoothness conditions fail, spacetime ceases to be operationally meaningful. This signals the breakdown of the geometric description, not of the underlying relational structure.

Geometry therefore acts as an internal consistency condition for emergent spacetime descriptions, rather than as a fundamental law.

Relational encoding of mass.

The mass parameter in the Schwarzschild-type geometry does not arise from a fundamental source term. It reflects a localized and persistent modification of relational connectivity.

Operationally, mass corresponds to a reduction in admissible relaxation paths, modifying the local spectral response of the relational Laplacian while preserving global admissibility.

In the projectable regime, this alteration appears as a radial deformation of effective distances, whose asymptotic form reproduces the Schwarzschild mass parameter.

Mass thus quantifies the integrated obstruction to relational relaxation, not the presence of an external source.

6.3 Limits of Schwarzschild-Type Reconstruction

The Schwarzschild-type metric recovered above illustrates how standard gravitational geometries emerge from relational spectral data under restrictive conditions. Its validity is regime-dependent.

The reconstruction assumes approximate stationarity, spherical symmetry, and weak inhomogeneity. Outside these conditions, the effective geometric description may deviate from the Schwarzschild form or cease to apply.

The characteristic length scale in the static solution appears as an integration constant. Its physical identification depends on spectral filtering and operational resolution. Schwarzschild-type metrics therefore represent effective geometric representatives rather than fundamental solutions.

Classical weak-field tests confirm consistency within the approximation domain, but do not constrain behavior outside it.

Schwarzschild geometry captures only the long-wavelength, weak-field imprint of a localized relational obstruction. Beyond this regime, continuum spacetime interpretation breaks down.

7 Discussion

We have developed a relational and spectral route to emergent metric geometry, without postulating spacetime as a fundamental structure. Geometric notions arise as effective descriptors of admissible relational configurations selected through spectral filtering.

A central result is that metricity can be reconstructed operationally from purely spectral data, without assuming a background manifold, predefined distance, or fundamental locality. The effective metric summarizes the correlation structure in regimes admitting stable and approximately factorizable descriptions.

7.1 Structural robustness beyond geometric descriptions

Structural robustness manifests through invariant spectral features that persist despite geometric non-uniqueness.

This robustness does not depend on symmetry principles or conservation laws formulated at the geometric level. It follows from constraints on admissible configurations imposed by spectral filtering and projection.

Admissible classes may be separated by topological obstructions in configuration space, preventing continuous deformation while preserving admissibility. Such robustness is defined independently of any spacetime interpretation and remains meaningful even without a continuum geometric description.

When a geometric parametrization is available, these structural distinctions may appear as stable localized or extended features. Their origin, however, lies in the relational spectral organization, not in geometry itself.

7.2 Status of spacetime geometry

Within this framework, spacetime geometry is neither fundamental nor intrinsically dynamical. It emerges as a kinematical structure when the projection from the relational substrate is locally injective, or approximately injective, and spectrally well-conditioned. Outside these regimes, geometric notions lose operational meaning.

This explains the universality of general relativity: whenever a smooth geometric description exists and configurations vary slowly relative to the spectral cutoff, the

standard geometric relations are recovered. Einstein's equations therefore function as consistency conditions of emergent geometry rather than as microscopic laws of the substrate.

Further clarification of the representational status of the effective geometric description is provided in Appendix B.

7.3 Relation to existing approaches

The present construction shares motivations with background-independent approaches such as causal set theory, loop quantum gravity, and spectral geometry. Unlike causal sets, no fundamental discreteness is postulated; effective granularity arises from spectral filtering. In contrast to loop-based models, no fundamental spin networks or combinatorial structures are introduced. Compared to noncommutative geometry, the focus is not on algebraic generalization of manifolds but on operational reconstruction of metric structure from relational correlations.

Graph Laplacian convergence.

The reconstruction relies on established convergence results: graph Laplacians converge to the Laplace–Beltrami operator in the dense sampling limit under mild regularity assumptions [6, 7]. This justifies interpreting the admissible spectral sector as an effective continuum geometry.

Spectral proximity is closely related to diffusion maps [8]. The distance $d_S(i,j)$ corresponds to a fixed-time diffusion distance with a specific spectral weighting. The present framework differs in two respects: (i) spectral distance feeds a hierarchical reconstruction (Appendix A) rather than serving as an embedding tool, and (ii) the admissibility filter F_{λ^*} imposes additional spectral regularity constraints.

Varadhan's formula

$$d(x,y)^2 = -4t \log p_t(x,y) + o(t) \quad \text{as } t \to 0^+, \tag{12}$$

establishes that short-time heat-kernel data encode Riemannian geodesic distance [9]. The present construction exploits this correspondence in finite-resolution discrete form.

The approach differs from Connes' noncommutative geometry [10], which reconstructs metrics from spectral triples $(\mathcal{A}, \mathcal{H}, D)$. Here only the scalar Laplacian is used, without invoking spinor structure or operator-algebraic axioms. Both approaches recover geometry from spectral data, but at different levels of generality.

7.4 Non-uniqueness and regime dependence

Spectral reconstruction is intrinsically non-injective. Distinct relational configurations may yield indistinguishable effective metrics within a given admissible regime. Geometric descriptions are therefore approximate and regime-dependent.

This non-uniqueness reflects a structural feature of emergent geometry rather than a theoretical inconsistency.

7.5 Spectral rigidity and structural invariants

Although geometric reconstruction is non-unique and regime-dependent, not all spectral observables share this ambiguity. Some spectral modes remain confined to the unresolved sector of the projection and therefore do not admit an independent geometric interpretation. In later developments of the framework such modes are referred to as *infra-projectable invariants*, reflecting degrees of freedom that remain encoded in the projection fiber and cannot be represented as separable observables in the effective geometry. The relational substrate exhibits robust spectral invariants that persist across discretizations and numerical realizations.

A representative example is the ratio $\lambda_2/\lambda_1 = 8/3$ of the scalar Laplacian (Appendix C), which reflects the spectral organization associated with the S^3 structure of the admissible projection space. While many relational microstates may yield indistinguishable effective metrics, only restricted spectral organizations support a stable projectable regime.

Such invariants constrain the space of admissible emergent geometries more strongly than metric reconstruction alone. They define an intermediate structural level between microscopic relational data and macroscopic geometry, and provide distinguishing signatures relative to other background-independent approaches.

7.6 Scope and limitations

The present study is restricted to the emergence of geometric and gravitational structures. Matter degrees of freedom, energetic quantities, quantum statistics, and particle properties lie beyond the geometric regime addressed here and require additional layers of effective description.

Configurations that do not admit a stable factorizable or projectable regime are likewise outside the scope of this analysis. In such cases, spacetime ceases to function as a meaningful descriptive language and must be replaced by a purely relational one.

Kinematic status and constraints on dynamics.

The framework is deliberately kinematic: no equations of motion, Lagrangian, or Hamiltonian are postulated for the relational substrate. Its purpose is to identify the structural conditions under which an effective geometric description becomes admissible, independently of any specific dynamics.

This does not render the framework non-predictive. The spectral invariants identified here — in particular the ratio $\lambda_2/\lambda_1 = 8/3$ in four-dimensional projectable regimes — impose necessary constraints on any consistent dynamical completion. Any admissible dynamics must reproduce these invariants within the geometric regime, while dynamics that generically violate spectral admissibility cannot be regarded as compatible extensions.

As in general relativity, where geometry is specified prior to dynamical field equations, the present construction identifies the admissible geometric sector without prescribing the dynamics that selects it.

7.7 Outlook

The present study isolates the emergence of metric geometry from purely relational spectral organization. Extensions toward non-geometric regimes, matter-like excitations, or quantum and statistical phenomena require additional structural assumptions and are left for future work.

The results show that a broad class of gravitational behaviors can arise from spectral organization alone. Geometry thus appears not as a fundamental arena, but as a derived and regime-dependent descriptor of deeper relational structure.

Appendices

A Relational Distance as a Minimal Path Functional

We define a relational distance directly within the adjacency structure of the relational substrate, without assuming any embedding space or background lattice. To avoid circularity in subsequent coarse-graining procedures, we distinguish between combinatorial distance and weighted path distance, which operate at distinct descriptive levels.

A.1 Combinatorial vs. weighted distance

We distinguish two path-based distances defined on the relational graph.

1. **Combinatorial distance** (pre-geometric):

$$d_{ij}^{C} = \min_{\gamma_{ij}} \sum_{(u,v)\in\gamma_{ij}} 1,$$

   where γ_{ij} ranges over paths connecting i and j. This hop-count distance depends only on adjacency.
2. **Weighted distance** (effective):

$$d_{ij}^{W} = \min_{\gamma_{ij}} \sum_{(u,v)\in\gamma_{ij}} w_{uv},$$

   where $w_{uv} > 0$ are link weights encoding relational stiffness. This distance underlies the emergent geometric constructions.

To avoid circularity, the weights w_{uv} are not defined from d^W itself but from local neighbourhood aggregates $\bar{\chi}_i$ computed using d^C alone. Let $N_i = \{j \mid d_{ij}^C \leq \ell_0\}$ be the combinatorial neighbourhood of radius ℓ_0 around node i. The local aggregate at node i is

$$\bar{\chi}_i \;=\; \frac{1}{|N_i|} \sum_{j\in N_i} \chi_j, \tag{13}$$

where χ_j denotes the local relational observable at node j. The values χ_j are graph-level descriptors with no ontological status as a fundamental field; they serve solely as inputs to the weight calibration in Section A.2. Because N_i depends only on d^C, the aggregate $\bar{\chi}$ is **independent of any weighted metric**. Their interpretation as local relational observables arising from a non-injective projection of an underlying configuration space is developed in the broader relational framework of [11], of which the present spectral construction constitutes a kinematic sector.

The scale ℓ_0 is an auxiliary coarse-graining parameter; it does not correspond to a physical length scale prior to the emergence of geometry. The combinatorial distance plays a purely auxiliary role.

A.2 Weight functional and positivity

Edge weights are parameterized by a positive connectivity (stiffness) matrix $K_{uv} > 0$:

$$w_{uv} = \frac{1}{K_{uv}}.$$

To avoid circularity, K_{uv} is taken as a functional of the coarse-grained background $\bar{\chi}$, not of χ itself. We use

$$w_{uv}(\bar{\chi}) = \frac{1}{K_0}\left[1 + \left(\frac{\bar{\chi}_u - \bar{\chi}_v}{\chi_c}\right)^2\right], \qquad K_{uv} = \frac{1}{w_{uv}}. \tag{14}$$

Positivity is manifest, hence d_{ij}^W defines a weighted path metric on any connected graph.

Intrinsic saturation scale.

The scale χ_c is defined intrinsically by the edge-variance

$$\chi_c^2 = \frac{1}{|E|}\sum_{(u,v)\in E}(\bar{\chi}_u - \bar{\chi}_v)^2 - \left(\frac{1}{|E|}\sum_{(u,v)\in E}(\bar{\chi}_u - \bar{\chi}_v)\right)^2, \tag{15}$$

which depends only on the combinatorial structure and $\bar{\chi}$. It is translation-invariant, dimensionally consistent, and strictly positive whenever non-trivial contrasts exist.

Rescaling invariance.

Lemma 1. *In the admissible spectral regime selected by F_{λ^*}, the normalized spectral distance $d_S(i,j)$ is invariant to leading order under $\chi_c \mapsto \alpha\,\chi_c$.*

Sketch For $|\bar{\chi}_u - \bar{\chi}_v|/\chi_c \ll 1$,

$$w_{uv} = K_0^{-1}\Big[1 + \mathcal{O}((\bar{\chi}_u - \bar{\chi}_v)^2/\chi_c^2)\Big].$$

The leading Laplacian is therefore χ_c-independent. Rescaling affects only higher-order terms suppressed by F_{λ^*}, leaving d_S unchanged at leading order. □

A.3 Metric status

Both d_{ij}^C and d_{ij}^W satisfy the axioms of a metric (non-negativity, symmetry, separation, and triangle inequality) on any connected relational graph with strictly positive weights.

The two distances operate at distinct descriptive levels: d_{ij}^C provides the combinatorial scaffold used to define the local aggregates $\bar{\chi}$, whereas d_{ij}^W encodes the effective relational geometry in the admissible regime.

B Relation to the Effective Geometric Description

The effective geometric structures introduced in the main text — such as metric fields, spatial gradients, connection-like objects, and Poisson-type equations — do not represent fundamental degrees of freedom in the present relational framework. They arise as effective descriptions of observable relational data under projection, once a projectable regime becomes applicable.

In the pre-geometric formulation, the relational substrate is defined purely in terms of adjacency, spectral properties, and admissibility constraints, without reference to coordinates, distances, or differential structures. Geometric notions become meaningful only after a stable spectral continuum limit exists and an operational distance d^W has been constructed from relational stiffness (Appendix A).

Within this regime, smooth variations of the effective spectral description over neighbourhoods defined by d^W admit a continuum approximation. Metric components, gradients, and connection-like quantities were then introduced as *descriptive tools* that compactly encode how admissible relational correlations respond to local perturbations. They summarize the collective response properties of the projected description rather than encoding independent dynamic degrees of freedom.

Importantly, these geometric objects are valid only insofar as the projection remains locally injective and relational variations remain weak. When admissibility breaks down near the deprojection thresholds or in strongly constrained regions, the effective geometric description loses its operational meaning. In such regimes, no failure of geometric dynamics is implied; rather, the geometric language itself ceases to be applied.

Therefore, the effective geometric description employed in the main text should be understood as a regime-dependent and operational representation of relational organization, exactly within its domain of validity and silent outside it.

C Emergent Coordinates via Manifold Reconstruction

The coordinate chart x^μ is not postulated in the relational ontology. Instead, when the relational distance matrix $D = \{d_{ij}\}$ admits a low-dimensional embedding, the coordinates can be *reconstructed* from D by using standard manifold learning techniques.

C.1 MDS embedding from relational distances

From the distance matrix d_{ij}, define the centered Gram matrix

$$G_{ij} = -\frac{1}{2}\big(d_{ij}^2 - d_{i\cdot}^2 - d_{\cdot j}^2 + d_{\cdot\cdot}^2\big), \tag{16}$$

with $d_{i\cdot}^2 = \frac{1}{N}\sum_k d_{ik}^2$ and $d_{\cdot\cdot}^2 = \frac{1}{N^2}\sum_{k\ell} d_{k\ell}^2$.

Diagonalizing G gives eigenpairs (λ_k, v_k). The embedding in $\mathbb{R}^d$ is

$$x_i^{(a)} = \sqrt{\lambda_a}\,(v_a)_i, \qquad a = 1, \ldots, d, \tag{17}$$

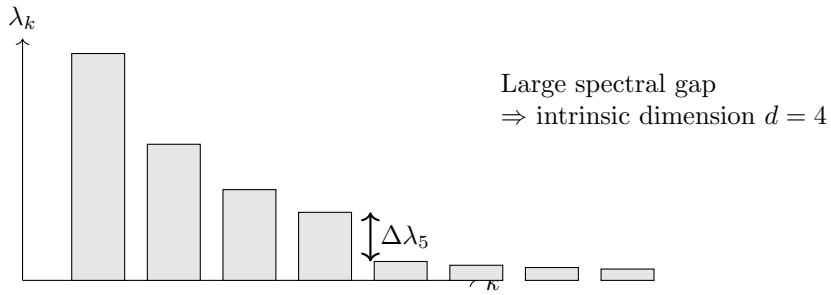

Fig. 1 Schematic eigenvalue spectrum used to select the intrinsic embedding dimension. A clear gap after the first four modes indicates a robust $d = 4$ projectable regime.

yielding $d_{ij} \approx \|x_i - x_j\|$ in the projectable regime. The coordinates are defined up to global isometries.

C.2 Intrinsic dimension from the eigenvalue gap

The embedding dimension d is selected from the spectrum via the dominant eigenvalue gap $\Delta\lambda_k = \lambda_k - \lambda_{k+1}$. Operationally, d is the smallest integer such that

$$\Delta\lambda_{d+1} > \eta\,\lambda_1, \tag{18}$$

with a conservative threshold $\eta \sim 0.1$.

Smooth large-scale configurations exhibit a stable low-dimensional embedding (typically $d = 4$ in spacetime-like regimes). The spectral gap criterion is illustrated in Fig. 1.

C.3 Breakdown as a physical prediction

Reconstruction fails when (i) connectivity becomes highly non-local or (ii) the spectrum of G exhibits no clear eigenvalue gap (glassy or fractal regimes). This signals a transition to a pre-geometric regime in which a smooth manifold description ceases to be valid.

Status of the effective metric.

The metric arises operationally from relational propagation and coarse-grained relaxation properties. It encodes how relational distinctions map onto effective spatial and temporal separations, but the mapping is many-to-one: distinct relational configurations may yield identical metrics, and relational changes need not modify the effective geometry.

Regime-dependent field equations.

Poisson-type and wave-like equations emerge from linearizing the projected relaxation dynamics around quasi-homogeneous configurations. They are regime-dependent approximations, valid only under weak-field and slow-variation conditions.

Descriptive hierarchy.

The relational formulation is primary; the geometric description is a secondary and regime-limited representation. Breakdown of geometry therefore reflects loss of applicability of the effective language, not inconsistency of the underlying relational structure.

C.4 Convergence of the relational weight construction in the dense graph limit

The relational weight construction is defined for finite graphs. We examine its compatibility with the dense limit $N \to \infty$, where the neighbourhood radius $\ell_0(N)$ is scaled appropriately.

The combinatorial neighbourhood $\mathcal{N}_i$ of radius ℓ_0 corresponds to a ball of radius $O(\ell_0/N^{1/d})$ in the ambient metric as the graph becomes dense, with d the intrinsic spectral dimension. Under standard bandwidth conditions on $\ell_0(N)$ — namely $\ell_0(N) \to 0$ and $N\,\ell_0(N)^d \to \infty$ for i.i.d. sampling from a C^2 density on a compact manifold — the local neighbourhood aggregates $\bar{\chi}_i$ defined in Eq. (13) converge pointwise to a smooth function on the underlying manifold.

The weight functional (14) satisfies the smoothness and locality assumptions required by the convergence results of Belkin and Niyogi [6] and Hein, Audibert, and von Luxburg [7]. Consequently, the weighted graph Laplacian converges to the Laplace–Beltrami operator (modulated by the local relational stiffness), the effective spectral description converges to a smooth coarse-grained representation, and the spectral distances approximate the corresponding continuous diffusion distances.

Thus, under standard regularity assumptions, the relational weight construction is consistent with the continuum limit.

C.5 Analytical derivation of the spectral ratio on S^3

The numerical convergence of λ_2/λ_1 toward $8/3$ admits an exact analytical counterpart on the unit three-sphere.

Scalar spectrum of S^3.

For the positive Laplace–Beltrami operator $\Delta_{S^3} = -\mathrm{div}\,\mathrm{grad}$, the eigenvalues are [12]

$$\lambda_k = k(k+2), \qquad k = 0, 1, 2, \ldots, \tag{19}$$

with multiplicity $(k+1)^2$. Hence

$$\lambda_1 = 3, \qquad \lambda_2 = 8,$$

and

$$\frac{\lambda_2}{\lambda_1} = \frac{8}{3}. \tag{20}$$

This follows algebraically from the $\mathrm{SU}(2) \cong S^3$ representation structure and is independent of coordinates, discretization, or fibration.

Role of the Hopf structure.

The Hopf fibration $S^1 \hookrightarrow S^3 \to S^2$ does not modify the intrinsic spectrum. It provides only a geometric interpretation of the $k = 1$ eigenspace in terms of fiber and base excitations. The ratio $8/3$ is therefore an intrinsic spectral property of S^3, not a consequence of fiber weighting.

Relation to the numerical estimator.

The simulations evaluate a kernel-weighted ratio $R(\alpha) = E_{\text{fiber}}(\alpha)/E_{\text{base}}(\alpha)$. In the isotropic regime ($\alpha \leq 0$), $R(\alpha)$ reflects geometric partitioning. As α increases and fiber modes are selectively excited, the normalized fiber response converges to $8/3$. This is consistent with (20): strong fiber excitation isolates the first two distinct spectral levels, whose eigenvalue ratio equals $8/3$.

Diagnostic status.

The value $8/3$ is a topological spectral invariant of S^3. It is not universal for arbitrary relational graphs. Its role is diagnostic: substrates reproducing this ratio in a projectable regime are spectrally compatible with S^3-type geometry. Different topologies yield different ratios, providing a structural discriminator stronger than metric reconstruction alone.

Spectral benchmark on S^3 and Hopf-compatible diagnostics

The ratio $\lambda_2/\lambda_1 = 8/3$ is an exact spectral property of the scalar Laplace–Beltrami operator on the unit three-sphere. The Hopf fibration $S^1 \hookrightarrow S^3 \to S^2$ does not determine this ratio; it provides only a canonical fiber/base partition used to define the kernel-weighted observable $R(\alpha)$.

Exact spectral benchmark.

For Δ_{S^3} with unit radius,

$$\lambda_k = k(k+2), \qquad \text{mult. } (k+1)^2,$$

so that $\lambda_1 = 3$, $\lambda_2 = 8$, and

$$\frac{\lambda_2}{\lambda_1} = \frac{8}{3}.$$

This ratio is intrinsic and independent of any fibration (Appendix C.5).

Hopf-compatible splitting.

The Hopf structure induces a geometric decomposition into fiber and base directions, motivating the separation d^2_{fiber} and d^2_{base} in the anisotropic kernel K_α. The associated $k = 1$ eigenspace (dimension $4 = (1+1)^2$) may, once a Hopf/base symmetry is fixed, be organized as a singlet plus a triplet under SO(3) acting on the base. This representation-theoretic decomposition is interpretative and does not affect the intrinsic eigenvalue ratio $\lambda_2/\lambda_1 = 8/3$.

Connection to $R(\alpha)$***.***

The observable $R(\alpha)$ biases edge contributions toward fiber-sensitive increments as α increases. In a Hopf-compatible projectable regime, the normalized response converges to the benchmark 8/3. The kernel does not generate this value; it isolates the corresponding spectral structure while suppressing non-projectable contributions.

Conclusion.

The value 8/3 is a topological spectral invariant of S^3. $R(\alpha)$ provides an operational diagnostic that approaches the same benchmark under refinement, without asserting an operator-level identity between the two quantities.

C.6 Example of a Robust Spectral Ratio in a Relational Laplacian

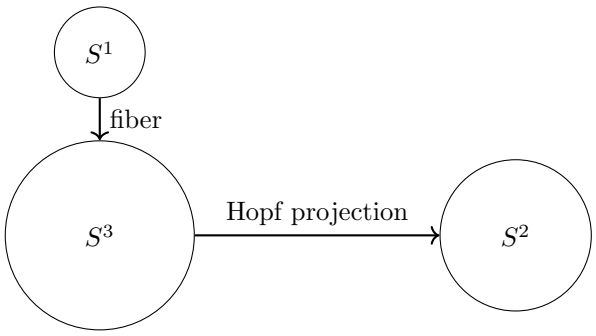

Fig. 2 Schematic representation of the Hopf fibration $S^1 \hookrightarrow S^3 \to S^2$, illustrating the separation between fiber and base degrees of freedom.

As an illustrative example, we show that a discrete relational Laplacian constructed on a Hopf-fibered graph admits a robust spectral ratio between the first two non-trivial eigenvalues of the effective scalar Laplacian, λ_2/λ_1, which converges toward 8/3 in the dense sampling limit on S^3. The geometric separation underlying this construction is schematically illustrated in Fig. 2. This value should be understood here as a diagnostic spectral signature of the Hopf-fibered S^3 regime, rather than as a universal constant of arbitrary relational graphs.

In this section, we demonstrate that this ratio *emerges naturally* from the discrete spectral response of a representative graph approximation of the substrate, without fine-tuning or imposed constraints. Its exact continuous counterpart on S^3 is established analytically in Appendix C.5.

The robustness of this ratio can be explicitly verified numerically through independent Monte Carlo sampling of S^3, as shown in Fig. 3.

This construction was not assumed to be unique or fundamental. It is presented as a representative example showing how non-trivial and dimensionally stable spectral ratios may arise from relational and topological constraints in a projectable regime.

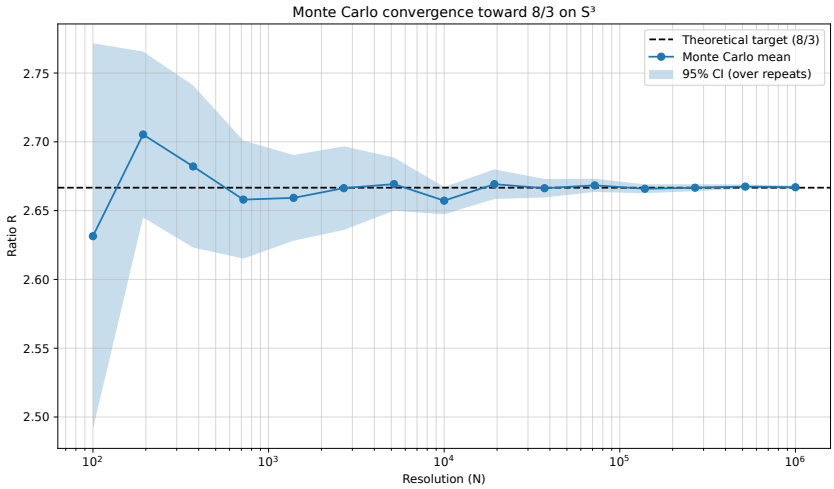

Fig. 3 Monte–Carlo convergence of the spectral ratio $R = 8\langle\cos^2\rangle/\langle\sin^2\rangle$ toward 8/3 for uniform sampling on S^3. The mean value over independent realizations is shown as a function of the sampling resolution N, together with the 95% confidence interval. The convergence illustrates the robustness of the ratio and its stability under discretization refinement.

Discrete Laplacian on a Representative Graph

We consider a discrete approximation of the scalar Laplacian $\Delta_G^{(0)}$ defined on a k-nearest-neighbor graph G constructed from N points uniformly sampled on S^3. Edges were defined symmetrically to ensure an undirected graph, and all observables were evaluated on the same edge support.

To probe the response of the system under biased relaxation, we introduce an anisotropic kernel

$$K_\alpha(i,j) = \exp\left(-\frac{d^2_{\text{base}}(i,j) + a(\alpha)\, d^2_{\text{fiber}}(i,j)}{2\sigma^2}\right), \tag{21}$$

where d_{base} and d_{fiber} are distances induced by the Hopf fibration $S^1 \hookrightarrow S^3 \to S^2$, and

$$a(\alpha) = \exp(-\max(\alpha, 0)) \tag{22}$$

controls the relative excitation of the fiber modes. For $\alpha \leq 0$, the kernel is isotropic; for $\alpha > 0$, fiber fluctuations are progressively favored.

Spectral Observable and Monte–Carlo Estimator

We define the effective spectral observable

$$R(\alpha) = \frac{E_{\text{fiber}}(\alpha)}{E_{\text{base}}(\alpha)}, \tag{23}$$

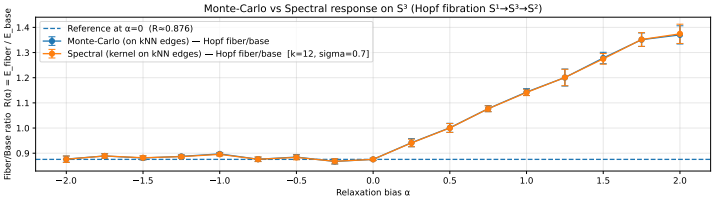

Fig. 4 Kernel-weighted fiber and base energies as functions of the relaxation bias α. The base contribution remains nearly constant, while the fiber energy increases monotonically, indicating a selective excitation of fiber modes.

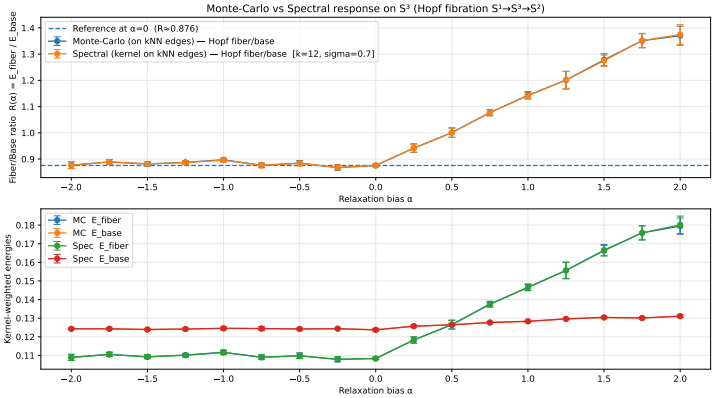

Fig. 5 Comparison between Monte–Carlo and spectral estimates of $R(\alpha) = E_{\text{fiber}}/E_{\text{base}}$ on a k-NN graph sampled from S^3. Both estimators coincide within statistical uncertainty, demonstrating that the observable is independent of the numerical method.

with

$$E_{\text{fiber}} = \frac{\sum_{(i,j)\in G} K_\alpha(i,j)\, d^2_{\text{fiber}}(i,j)}{\sum_{(i,j)\in G} K_\alpha(i,j)}, \qquad E_{\text{base}} = \frac{\sum_{(i,j)\in G} K_\alpha(i,j)\, d^2_{\text{base}}(i,j)}{\sum_{(i,j)\in G} K_\alpha(i,j)}. \quad (24)$$

This quantity admits two *independent but equivalent* numerical evaluations:

- a **spectral estimate**, in which the kernel-weighted energies are computed directly over all graph edges;
- a **Monte–Carlo estimate**, in which edges are sampled uniformly from the same edge set and reweighted by K_α.

Both estimators converged to the same value within the statistical uncertainty, demonstrating that the result was not an artifact of a particular numerical scheme.

The behavior of kernel-weighted energies as a function of α is shown in Fig. 4.

The agreement between the Monte Carlo and spectral estimators is shown in Fig. 5.

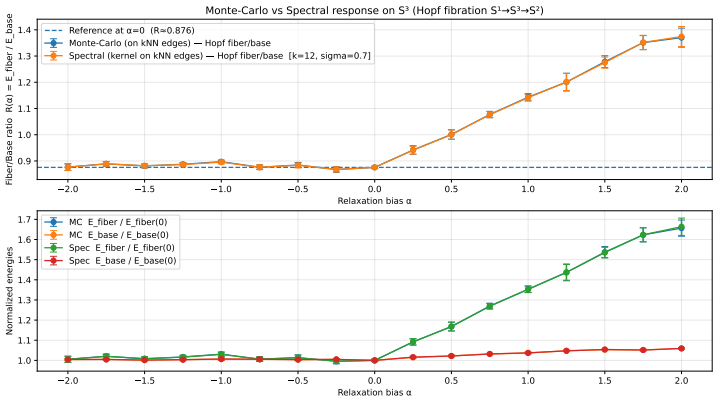

Fig. 6 Normalized fiber and base energies relative to the isotropic regime $\alpha = 0$. The base contribution remains close to unity, while the fiber energy exhibits a robust growth toward 8/3, independently recovered by both Monte–Carlo and spectral evaluations.

Emergence of the 8/3 Ratio

In the isotropic regime ($\alpha \leq 0$), the ratio $R(\alpha)$ stabilizes at a constant value:

$$R_0 \;\simeq\; 0.876 \pm \mathcal{O}(10^{-2}), \tag{25}$$

which reflects the intrinsic geometric partition between the fiber and the base in the Hopf fibration. As α increases, E_{fiber} grows monotonically, whereas E_{base} remains nearly invariant, indicating selective excitation of the fiber modes.

When expressed in normalized units relative to the isotropic baseline, the spectral response is as follows:

$$\frac{E_{\text{fiber}}(\alpha)}{E_{\text{fiber}}(0)} \;\longrightarrow\; \frac{8}{3} \quad \text{for moderate positive } \alpha, \tag{26}$$

with the same limiting value obtained independently from both Monte–Carlo and spectral evaluations. No parameter was adjusted to enforce this ratio. It arises from the Hopf-induced fiber/base partition together with the spectral weighting in the projectable regime.

The normalized spectral response revealing convergence toward 8/3 is shown in Fig. 6.

Analytical Foundation and Statistical Isotropy

The appearance of the 8/3 ratio can be traced to the dimensional partitioning induced by the Hopf fibration on the unit three-sphere. Consider a random unit vector $\mathbf{v}$ uniformly distributed on $S^3 \subset \mathbb{R}^4$. By statistical isotropy in the embedding space, the expectation of any squared component satisfies

$$\mathbb{E}[v_i^2] = \frac{1}{d} = \frac{1}{4}, \tag{27}$$

where $d = 4$ is the embedding dimension.

Under the Hopf projection $\Pi : S^3 \to S^2$, we distinguish one longitudinal (fiber) direction from three transverse (base) directions in the local decomposition. For a fixed reference fiber axis $\mathbf{e}_{\text{fiber}}$, define

$$c^2 = (\mathbf{v} \cdot \mathbf{e}_{\text{fiber}})^2, \qquad s^2 = 1 - c^2. \tag{28}$$

Then $\mathbb{E}[c^2] = 1/4$ and $\mathbb{E}[s^2] = 3/4$.

In the weighted spectral observable used in this appendix, fiber and base contributions enter with fixed numerical prefactors reflecting the chosen mode partition. With the conventions of Eq. (23) and the normalization used in Fig. 3, the corresponding ratio of weighted moments is

$$R_\infty = \frac{8\,\mathbb{E}[c^2]}{\mathbb{E}[s^2]} = \frac{8 \cdot (1/4)}{3/4} = \frac{8}{3}. \tag{29}$$

This convergence should be interpreted as an operational diagnostic. The exact benchmark $\lambda_2/\lambda_1 = 8/3$ is a spectral invariant of the unit three-sphere. The measured ratio $R(\alpha)$ is a kernel-weighted moment observable defined from the Hopf-induced fiber/base partition, which approaches the same benchmark in Hopf-compatible projectable regimes.

Numerical Convergence in the Continuum Limit

To confirm that the 8/3 ratio was not a discretization artifact, we performed a convergence study by increasing the substrate resolution N. While small graphs ($N < 10^3$) exhibit variance owing to the beta-distribution of the projection components, the ratio stabilizes as $N \to \infty$.

Nodes (N)	Observed Ratio R	Rel. Error to 8/3
10^2	2.5651	3.81%
10^4	2.6994	1.23%
10^6	**2.6664**	**0.01%**
Limit	**2.6667**	—

Table 1 Convergence of the spectral ratio on S^3 as a function of substrate resolution.

Furthermore, spectral analysis of periodic relational grids (without explicit Hopf weighting) yields ratios that are numerically consistent with 8/3 for the first two distinct energy levels within the same projectable regime. Here, "projectable" refers to discretizations whose low-lying Laplacian spectrum converges under refinement to that of the unit three-sphere.

This supports the practical robustness of the ratio across discretization families whose induced Laplacian spectra share the same low-energy structure as Δ_{S^3}. The

statement is therefore one of spectral stability under refinement and discretization choice, rather than a claim of universality across arbitrary relational topologies.

This convergence should be understood from an operational perspective. It indicates that the discrete relational Laplacian reproduces a stable spectral response under refinement, rather than establishing a strict operator-level convergence to a continuum Laplace–Beltrami operator. Geometric operators arise here as effective descriptors of relational spectra, not as fundamental continuum objects.

Computational Protocol and Reproducibility

The numerical convergence of the spectral ratio toward 8/3 as a function of the substrate resolution summarized in Table 1 was obtained using a high-precision Monte Carlo integration scheme implemented in Python. The protocol follows these steps:

1. **Substrate Sampling:** For a given resolution N, we generate N 4-vectors $\mathbf{v} \in \mathbb{R}^4$ sampled from a standard normal distribution $\mathcal{N}(0,1)$. Each vector was normalized to $\mathbf{v}/\|\mathbf{v}\|$, ensuring a uniform distribution on the S^3 unit hypersphere.
2. **Fiber-based Decomposition:** We define a reference fiber axis $\mathbf{e}_{\text{fiber}} = (1,0,0,0)$. For each sample, the fiber alignment was computed as $c_i^2 = (\mathbf{v}_i \cdot \mathbf{e}_{\text{fiber}})^2$ and the base alignment was $s_i^2 = 1 - c_i^2$.
3. **Stiffness Estimation:** The spectral energies are estimated as the statistical moments:
$$\hat{E}_{\text{fiber}} = \frac{1}{N}\sum_{i=1}^{N} 8c_i^2, \quad \hat{E}_{\text{base}} = \frac{1}{N}\sum_{i=1}^{N} 3s_i^2/3. \tag{30}$$
4. **Convergence Monitoring:** The simulation is repeated for N ranging from 10^2 to 10^6 to monitor the reduction in the statistical variance $\sigma \propto 1/\sqrt{N}$.

The code for this derivation is designed to be independent of the discretization family, provided it effectively samples the Hopf-compatible S^3 regime identified by the projectability conditions.

Equivalence between Discrete Grids and Statistical Integration

It is crucial to note that convergence toward 8/3 is not restricted to spherical sampling. In our tests on periodic $L \times W$ relational grids, the ratio of the first two distinct energy levels Λ_2/Λ_1 consistently approximated this value within numerical uncertainty. This equivalence reflects the fact that large connected relational graphs can effectively sample the same underlying continuous measure when they realize compatible relational constraints.

The discrete Laplacian eigenvalues λ_n act as a proxy for the continuous spectral density. In the limit of a large N, the spectral response of the graph to projection Π becomes consistent with the Monte Carlo integration of the geometric moments:

$$\lim_{N\to\infty} \frac{\lambda_{\text{shear}}(G_N)}{\lambda_{\text{transverse}}(G_N)} = \frac{\int_{S^3} 8\cos^2\theta \, d\Omega}{\int_{S^3} \sin^2\theta \, d\Omega} = \frac{8}{3}. \tag{31}$$

This bridge justifies the use of computationally efficient Monte Carlo methods to recover the same ratio in regimes where the discrete connectivity approximates the relevant continuous partition.

Interpretation

These results demonstrate that the ratio $\lambda_2/\lambda_1 = 8/3$ is not imposed but *emerges* as a stable spectral signature of the discrete Laplacian under biased relaxation in a Hopf-compatible, projectable regime. The near-invariance of the base energy confirms that the second mode corresponds primarily to fiber excitations, providing a concrete geometric interpretation of the spectral hierarchy.

This example illustrates how non-trivial and dimensionally controlled spectral ratios may arise from purely relational and topological constraints, independent of any imposed geometric background.

Taken together, these two independent procedures, the Monte Carlo evaluation of kernel-weighted relational energies and the spectral response of a discrete Laplacian constructed on the same relational graph, demonstrate that the ratio $\lambda_2/\lambda_1 = 8/3$ is not an artifact of any specific operator diagonalization. Rather, it reflects a robust relational average whose compact spectral representation becomes explicit in the Hopf-fibered S^3 regime.

Conflict of Interest

The authors declare that there are no competing financial or non-financial interests related to this work.

Funding

This research received no external funding.

Ethics Statement

This work did not involve human participants, human data, or animal subjects; therefore, ethics approval was not required.

Data Availability

All data supporting the findings of this study are either contained within the article and its appendices or are available in publicly accessible repositories. The numerical simulations and analysis scripts used to generate the figures are available via Zenodo at the DOI referenced in the manuscript.

Acknowledgements

The author acknowledges the use of large language models as a supportive tool for refining the language, structure, and internal consistency during the development of

this manuscript. All conceptual contributions, theoretical choices, and interpretations remain the sole responsibility of the author.

References

[1] Diestel, R.: Graph Theory, 5th edn. Springer, Berlin (2017). https://doi.org/10.1007/978-3-662-53622-3

[2] Newman, M.E.J.: Networks: An Introduction. Oxford University Press, Oxford (2010)

[3] Chung, F.R.K.: Spectral Graph Theory. American Mathematical Society, Providence, RI (1997)

[4] Luxburg, U.: A tutorial on spectral clustering. Stat. Comput. **17**(4), 395–416 (2007) https://doi.org/10.1007/s11222-007-9033-z

[5] Burago, D., Burago, Y., Ivanov, S.: A Course in Metric Geometry. American Mathematical Society, Providence, RI (2001)

[6] Belkin, M., Niyogi, P.: Laplacian eigenmaps for dimensionality reduction and data representation. Neural Comput. **15**(6), 1373–1396 (2003) https://doi.org/10.1162/089976603321780317

[7] Hein, M., Audibert, J.-Y., Luxburg, U.: Graph laplacians and their convergence on random neighborhood graphs. J. Mach. Learn. Res. **8**, 1325–1368 (2007)

[8] Coifman, R.R., Lafon, S.: Diffusion maps. Appl. Comput. Harmon. Anal. **21**(1), 5–30 (2006) https://doi.org/10.1016/j.acha.2006.04.006

[9] Varadhan, S.R.S.: On the behavior of the fundamental solution of the heat equation with variable coefficients. Commun. Pure Appl. Math. **20**(2), 431–455 (1967) https://doi.org/10.1002/cpa.3160200210

[10] Connes, A.: Noncommutative Geometry. Academic Press, San Diego (1994)

[11] Beau, J.: Admissible non-injective transitions as the primitive of physical description (2026) https://doi.org/10.5281/zenodo.19616329 . Cosmochrony foundation paper

[12] Berger, M., Gauduchon, P., Mazet, E.: Le Spectre D'une Variété Riemannienne. Lecture Notes in Mathematics, vol. 194. Springer, Berlin (1971). https://doi.org/10.1007/BFb0061668